

Review

# Advances in Carbon Nanomaterial–Clay Nanocomposites for Diverse Applications

Jayanta S. Boruah and Devasish Chowdhury \* 

Material Nanochemistry Laboratory, Physical Sciences Division, Institute of Advanced Study in Science and Technology, Guwahati 781035, India

\* Correspondence: devasish@iasst.gov.in

**Abstract:** Clay materials are widely used in sheet-type platforms with peculiar characteristics and diverse applications. However, due to some disadvantages—such as weak mechanical strength and low reactivity—they are often subjected to modifications. Such tuning leads to better output than pure clay materials. This review describes some of the clay hybrids in the form of nanocomposites with carbon nanomaterials. Generally, graphene oxide or its derivatives—such as reduced graphene oxide, carbon nanotubes, carbon dots, carbon nanoclusters, and polymeric components—have been utilized so far to make efficient clay composites that have applications such as catalysis, wastewater treatment for toxin removal, cargo delivery, stimulus-responsive advanced tools, optoelectronics, mechanically stable films for filtration, etc. It is interesting to note that nearly all of these applications tend to show the efficacy of modified clay nanocomposites as being significantly greater than that of pure clay, especially in terms of mechanical strength, loading capacity, increased surface area, and tunable functionality. According to the literature, the evidence proves the beneficial effects of these clay nanocomposites with carbon nanomaterials.

**Keywords:** nanocomposite; clay; carbon nanomaterial; adsorption; nanofiltration



**Citation:** Boruah, J.S.; Chowdhury, D. Advances in Carbon Nanomaterial–Clay Nanocomposites for Diverse Applications. *Minerals* **2023**, *13*, 26. <https://doi.org/10.3390/min13010026>

Academic Editor: Luciana Sciascia

Received: 6 November 2022

Revised: 15 December 2022

Accepted: 19 December 2022

Published: 23 December 2022



**Copyright:** © 2022 by the authors. Licensee MDPI, Basel, Switzerland. This article is an open access article distributed under the terms and conditions of the Creative Commons Attribution (CC BY) license (<https://creativecommons.org/licenses/by/4.0/>).

## 1. Introduction

Clay is a class of fine-grained natural soil material consisting mainly of aluminosilicates, sometimes with variable amounts of iron, magnesium, alkali metals, and alkaline earth metals, as well as other cations in different crystalline planes. Guggenheim and Martin (1995), as per the AIPEA guidelines, defined clay as a plastic material with a particular water content that tends to be hard once dried [1]. Along with natural clay, manmade clay is used, also known as synthetic clay. The components show the characteristic of plasticity with appropriate water concentration, which leads to permanent hardness once water is removed. On the other hand, clay minerals are those phyllosilicates or minerals that impart plasticity into the clay [2]. The planar hydrous phyllosilicate minerals are arranged in seven groups (serpentine–kaolin, talc–pyrophyllite, smectite, vermiculite, true mica, brittle mica, and chlorite) according to the type of silicate layer (1:1 or 2:1), the net layer charge, and the interlayer material that compensates for the layer charge. The non-planar hydrous phyllosilicates are classified according to the modulated components of the minerals [2]. Kaolinite, halloysite, nacrite, and dickite have a 1:1 layer composed of one octahedral and one tetrahedral sheet; these mineral belong to the serpentine–kaolin group [2,3]. The primary difference among the members is the position of the vacant site from layer to layer [2]. The remaining five groups belong to the clay minerals; their 2:1 layer is composed of two tetrahedral sheets and one octahedral sheet between them. All of the groups are varied in terms of the interlayer materials and octahedral characteristics present. Smectite clays include montmorillonite, bentonite, saponite, and hectorite as the main representatives, which are primarily 2:1 layer clays generated from the breakdown of soils, rocks, or volcanic ash. This type of layered clay consists of an octahedral sheet placed between two opposing

tetrahedral sheets. The interlayer materials—such as cations, hydrated cations, organic molecules, and hydroxide octahedral sheets—separate the layers. Kaolinite has a lamellar structure with the chemical formula  $\text{Al}_2\text{Si}_2\text{O}_5(\text{OH})_4$ , constructed in the order 1:1, where each separate layer represents a layer from  $\text{Si}_2\text{O}_5^{2-}$  tetrahedrons and alumina  $[\text{Al}_2(\text{OH})_4]^{2+}$  octahedrons, connected through mutual oxygen atoms bearing hydrogen bonds [4–6]. The main reactivity of kaolinite is governed by the location of hydroxyl groups (OH) in its structure [7,8]. Vermiculites are secondary minerals of the micas (biotites). Vermiculites' 2:1 layer charge is high and balanced by hydrated exchangeable cations in the interlayer [9], which possesses high cation-exchange capacity of weakly hydrated cations, viz.,  $\text{K}^+$ ,  $\text{NH}_4^+$ , and  $\text{Cs}^+$  [2,10].

Illite is the most common 2:1 layer silicate found in the deep sea. The chemical formula for illites is  $\text{K}_y\text{Al}_4(\text{Si}_{8-y},\text{Al}_y)\text{O}_{20}(\text{OH})_4$ , with  $1 < y < 1.5$ . Occasionally, charge imbalance directs the use of Ca and Mg in place of K. The interlayer cations (i.e., K, Ca, or Mg) prevent the entry of  $\text{H}_2\text{O}$  into the structure, making the clay non-expansive [2,11]. Illite group clays are also known as clay micas, and the most frequently used members of this group are illite, glauconite, and muscovite. They are generally produced as a result of alkaline weathering of rocks that are rich in potassium and aluminum (e.g., muscovite and feldspar).

Moreover, chlorites are hydrous 2:1 layered aluminosilicates that act as basic minerals in soils to generate vermiculite and smectite [2,12]. Chlorites are known to be non-expansive in nature because of their negligible water adsorption through the interlayer space. The octahedral sheet (in the 2:1 layer) and the interlayer hydroxide sheet mostly allow cations such as Mg, Al, and Fe. Small numbers of Cr, Ni, Mn, V, Cu, and Li cations are also present there. A substantial replacement of Si by Al cations is depicted in the tetrahedral sheet.

Apart from the phyllosilicates mentioned above, the soil clay may also include trace amounts of oxides, hydroxides, and hydroxy-oxides of elements such as Si, Al, and Fe, along with some weakly crystalline aluminosilicates [13]. Quartz and opal are two common Si oxides found in clay. Similarly, gibbsite ( $\text{Al}(\text{OH})_3$ ) and goethite ( $\text{FeOOH}$ ) are the most prevalent Al hydroxide and Fe mineral representatives in soil clay fractions, respectively. Volcanic soils contain allophane and imogolite, which are two weakly crystalline aluminosilicates.

As the structure and composition of clay materials are unique, their applications in various fields are attracting attention. Scholars have been using these materials in pure and composite states for a long time to explore their capabilities. Among others, bentonite is a very commonly used rock developed from colloidal and malleable clays—primarily montmorillonite, with lesser amounts of feldspar, cristobalite, and crystalline quartz [13]. Bentonites (3%–5%) act as bonding agent to bind sands into tunable forms for the casting of metals [14]. Due to its swelling capacity and very small size, bentonite functions as an efficient soil sealant. It causes a very low permeability barrier in the soil by filling the gaps, thereby swelling the interstices of the soil. Kaolin, also known as China clay, is a mineral combination of kaolinite, quartz, mica, feldspar, illite, and montmorillonite. Kaolinite is constructed of triclinic crystal sheets in the shape of a pseudo-hexagon. Interestingly, kaolin-coated papers have been employed in the production of cigarettes [15]. In fact, in the biomedical field, kaolinite is a well-known material for its good capacity to adsorb lipids, proteins, viruses, and bacteria [15,16]. It also contributes to platelet aggregation by activating factor XII, leading to plasma coagulation [17].

In water purification, clay filters demonstrate effectiveness for decontaminating water by removing microbes [18], chemicals [3], and heavy metals. These filters perform very efficient water filtration through adsorption/absorption, ion-exchange mechanisms, and molecular sieving [19].

In most of its applications, clay has been used in composite or nanocomposite forms rather than in a pure state due to its many advantageous properties when modified. Most of the earlier studies on composite preparation started with the utilization of clay frames as effective templates for making novel carbon structures [20–23]. Initially, intercalation of different monomers (e.g., furfuryl alcohol, acrylonitrile, and vinyl acetate) into the clay layers was attempted, followed by polymerization, which could result in graphite-like carbon

structures with interesting properties [24–26]. A possible structure of a representative clay carbon composite is shown in Figure 1 below.

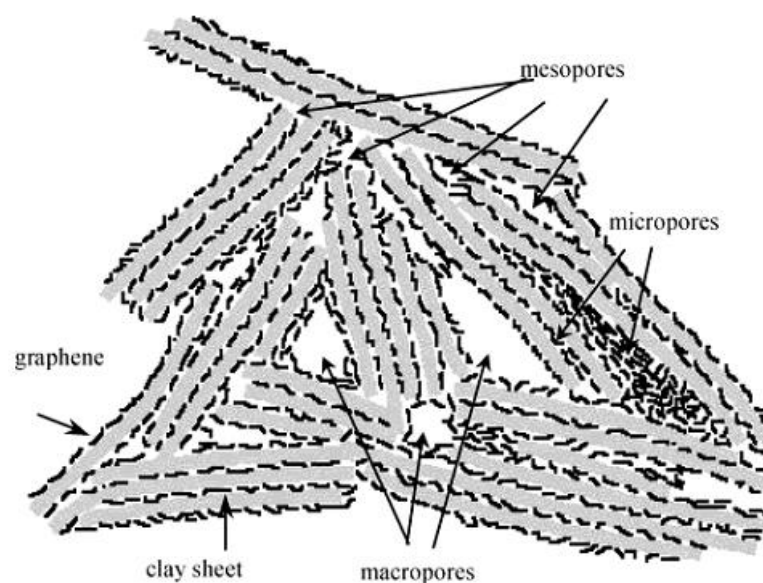


**Figure 1.** Schematic view of the probable architecture of a clay carbon composite (reproduced from ref. [27], copyright 2004, American Chemical Society).

The intercalation and ion-exchange characteristics of smectites offer simple routes for the inclusion of various precursors—mainly of carbon origin—between the layers. Thermal treatment results in clay–carbon hybrids where graphene sheets are assembled in dynamic ways, forming micropores, mesopores, and macropores [27]. These composites are applicable to many important applications, such as catalysis, gas separation, waste absorption, and in lithium batteries as anode materials [22,24,28]. Furthermore, the increased thermal stability of developed clay–carbon composites was investigated by a group of researchers, owing to the shielding effect of graphene present within the interlayer space covering the clay platelets [27].

As described above, many such composites of clay give rise to interesting functions in relevant areas, such as catalysis, sensing, biomedical implications, etc. Moreover, the use of carbon-based molecules to make such composites with clay provides multiple advantages in terms of reduced toxicity, increased biocompatibility, and green chemistry. Furthermore, the addition of nanotechnology to this area imparts manifold enhancement of the efficiency of the clay composites. Therefore, this review summarizes all types of carbon nanocomposites of clay, along with their routes of synthesis, properties, and applications to date.

## 2. Synthesis, Properties, and Applications of Different Carbon Nanocomposites of Clay

Due to the unique structures of clays and their derivatives as nanocomposites, they display exceptional reactivity, significant optical properties, and strong mechanical characteristics. Based on their properties and areas of application, they can be divided into four main classes, as discussed below to provide an insight into the hybrids. Figure 2 shows a schematic view of the uses and properties of clay–carbon nanomaterial composites.

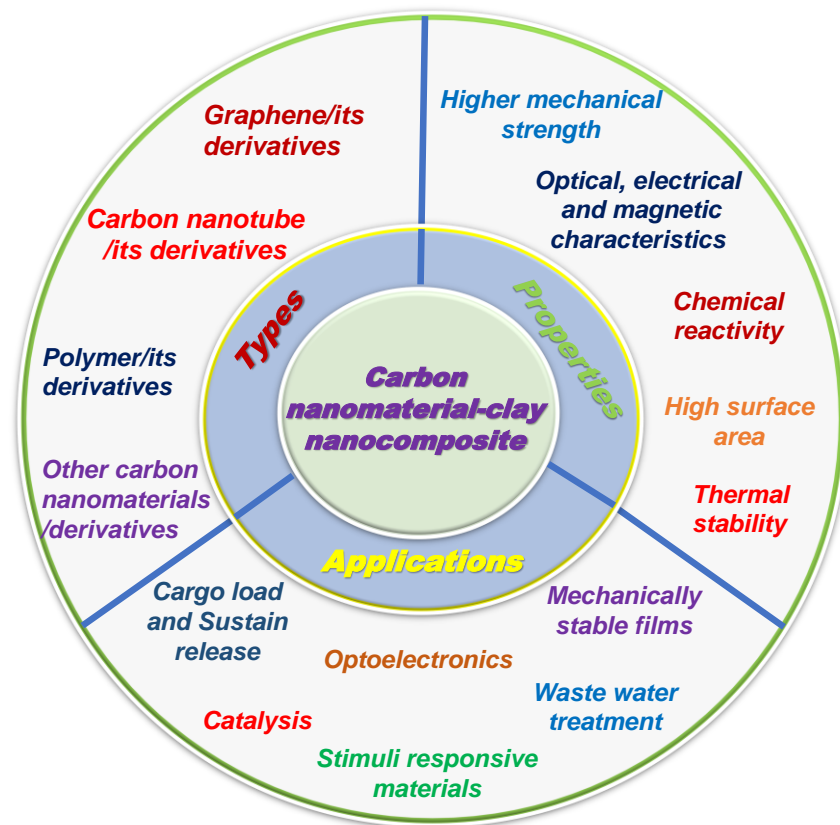


**Figure 2.** Schematic view of carbon nanomaterial–clay nanocomposites, along with their types, properties, and applications.

### 2.1. Graphene-Based Clay Nanocomposites

Among various carbon-based materials, graphene and graphene oxide have been a hot topic for scholars working in the field of clay chemistry. The easy route of preparation and smooth electronic movement in the graphene oxide (GO) structure are the leading factors driving their use in such types of nanocomposite. There are a number of earlier reports showing the formation of such nanocomposites from clay and GO, which are useful for dynamic applications. As a contribution, our group has developed one such composite, made up of bentonite clay and GO via three different methods [29]. After successful formation, it was applied as a photocatalyst for the degradation of a cationic dye (methylene blue). The selectivity of the catalyst was confirmed using two anionic dyes (methyl orange and eosin yellow), for which it could not show such activity. The photocatalytic activity was compared with that of pure clay or graphene oxide and found to be better for the nanocomposite.

Another composite hydrogel was reported consisting of graphene oxide, hectorite clay, and poly(N,N-dimethylacrylamide) (PDMAA), which possessed enhanced mechanical properties along with fast self-healing capability in the presence of near-infrared (NIR) radiation [30]. The higher mechanical strength of the hydrogel was attributed to the crosslinking between clay sheets and chains of PDMAA. Here, GO acts as a crosslinking agent and NIR absorber to effectively transform the NIR energy to thermal energy in the hydrogel, resulting in fast self-healing.

Clay nanocomposites are also used in sensing applications with GO. A gas sensor was developed with kaolin–graphene oxide nanocomposites [31]. The main driving force to fabricate the nanocomposite was 3-aminopropyltriethoxysilane (APTES), which binds GO flakes to kaolin. The sheet resistance measurements suggest the conductive nature of the nanocomposite after thermal annealing. Based on the variation in the conductance of the nanocomposite films, electrical gas sensors for the detection of  $\text{NH}_3$  and  $\text{HNO}_3$  were

devised. These devices were superior in terms of sensitivity as compared to multilayer GO films that were thermally annealed. The thermally reduced GO played a tremendous role in the sensitivity of the gas sensors.

Such composites have been utilized in many other applications. Among them, catalyst formation for organic synthesis is becoming an interesting area to explore. For that, a clay–graphene oxide nanocomposite was successfully prepared for application in a multi-component one-pot organic synthesis, called the Biginelli reaction [32]. The synthesis of 3,4-dihydropyrimidinones through this catalyst could produce higher yields. In fact, the partial GO reduction upon the incorporation of clay under heat treatment was confirmed by the XRD pattern of the nanocomposite.

Similar to GO, reduced graphene oxide has also been employed in the formation of nanocomposites with clay. For example, a reduced graphene oxide–montmorillonite (GCM) nanocomposite was fabricated for the adsorption of Cr(VI) from water [33]. The reductant used for the graphene oxide was ascorbic acid. It was noted that the adsorption was highly pH-dependent, and the maximum adsorptive capacity was recorded at pH 2. Pseudo-second-order kinetics was followed for the rate of the Cr(VI) adsorption. An adsorptive capacity of 12.86 mg g<sup>-1</sup> (20 °C) was found for Cr(VI), determined from the Langmuir isotherm model.

However, scholars are also trying to incorporate these nanocomposites in the green energy sector, particularly for hydrogen storage purposes. For instance, GO/reduced GO are well known for their hydrogen adsorption capacity of 0.68 wt % at 77 K and 1 bar, as reported by Srinivas et al.; thus, their composites must have improved capabilities for this type of energy storage [34]. With this motivation, clay–graphene nanomaterials were developed using precursors such as sucrose (caramel) and natural clays (montmorillonite and sepiolite) to evaluate their potential use in hydrogen storage from a green perspective [35]. The actual process involves the impregnation of the clay with aqueous caramel and thermal treatment without oxygen, producing graphene-like materials that are strongly bound to the silicate layer. The best performance of these nanocomposites for hydrogen storage was achieved at 298 K and 20 MPa, where 0.1 wt % excess hydrogen adsorption took place with respect to the total mass of the system, and a maximum of 0.4 wt % hydrogen was adsorbed with respect to the carbon mass.

It was noted that graphene oxides show aggregation during storage or application, reducing their performance. Hence, work has been carried out to modify GO with other moieties. One such example included the preparation of montmorillonite-modified pillared GO for improved adsorption of lead ions (Pb<sup>2+</sup>) and methylene blue (MB) [36]. The adsorption behavior of the nanocomposite was verified in both single and binary systems. Interestingly, the system possessed a larger BET specific surface area than that of pure GO. The maximum adsorption capacities in the single system for MB and Pb<sup>2+</sup> were 350 and 285 mg/g, respectively. In fact, the surface area and the maximum adsorption capacity of the system remained approximately constant, while the values for the GO dramatically decreased. For binary systems, the MB provided additional binding sites for Pb<sup>2+</sup> in water, thereby promoting its adsorption.

There are other reports also depicting varieties of such applications based on composites of graphene or its derivatives with clay. A few important examples are mentioned above, along with their characteristics and advantages.

## 2.2. Carbon Nanotube–Clay Nanocomposites

Along with GO, the other most frequently used carbon nanomaterial to make composites with clay is carbon nanotubes (CNTs). The sheet-type architecture of CNTs, arranged in cylindrical manner, makes them compatible with clay materials, imparting the composite with many suitable properties, such as increased surface area, reactivity adjustment, and nano-assisted optical properties. To begin with, scholars have used clay as a template for the growth of carbon nanotubes for a long time. One such example reported the successful development of multiwalled carbon nanotubes (MWCNTs) on clay (montmorillonite)

surfaces, attained via chemical vapor deposition of acetylene [37]. Based on the metal salt catalysts used (i.e.,  $\text{FeCl}_3 \cdot 6\text{H}_2\text{O}$ ,  $\text{Fe}(\text{NO}_3)_3 \cdot 9\text{H}_2\text{O}$ ,  $\text{Ni}(\text{NO}_3)_2 \cdot 6\text{H}_2\text{O}$ , and  $\text{Co}(\text{NO}_3)_2 \cdot 6\text{H}_2\text{O}$ ), clay–carbon nanotube composites of varying contents and quality were produced. Immobilized metal nanoparticles on the clay surfaces or at the edges served as the active sites for CNTs' development. The advantage of using of  $\text{Ni}(\text{NO}_3)_2$  is in attaining high quality or a low number of defects in the composite. Moreover, there is a simplified process to make unique 3D nanostructured fillers, in which intercalation of  $\text{Fe}_2\text{O}_3$  particles takes place to exfoliate the 2D clay platelets, and then 1D nanotubes are grown on the exfoliated surface [38]. The nanocomposite's formation reduces the step of purification during CNT synthesis. Furthermore, the enhancement of the activity of the nanostructured filler was demonstrated by including the CNT–clay hybrid in nylon 6. It was observed that through the incorporation of only 1 wt % nanocomposite filler, the modulus and tensile strength of the hybrid were significantly improved compared to neat nylon 6, by 290% and 150%, respectively. Researchers have also worked on the formation of clay–CNT hybrids, including the synthesis of homogenous multiwalled carbon nanotube–montmorillonite nanocomposites [39]. Their composition is such that the MWCNTs behave as a single nanotube, absorbed on the surface and edges of the montmorillonite sheets. The clay layers, having a highly negative charge, exhibit strong interactions with the aqueous dispersion of nanotubes, restricting the CNTs from aggregating. Thus, the resultant stability of CNTs offered by clay is able to separate the individual nanotubes from one another.

In fact, clay-assisted enhanced dispersion of CNTs was achieved in water, toluene, dimethylformamide, and ethanol through the formation of hybrids with anionic synthetic fluorinated mica, anionic sodium montmorillonite, and cationic layered double hydroxide [40]. Moreover, the aggregation behavior was controlled with such modification of CNTs.

The process has been improved further with CNT-based composites. In 2011, a mechanically robust and magnetic nylon-6 nanocomposite, supported by 1D CNTs and 2D clay nanoplatelets, was reported [41]. The MWCNTs utilized iron-oxide-immobilized clay nanoplatelets as substrates. The thermodynamically stable R-phase crystals of nylon 6 were successfully formed with the support of the nanohybrids, which had higher stiffness and hardness than the  $\gamma$ -form of nylon 6. It was also noted that the nanohybrid could prevent the transformation of the R-form to the  $\gamma$ -form. The residual iron oxide nanoparticles in the composite imparted the nylon-6 system with novel magnetic properties.

In the case of membrane research, this type of composite has been found to be useful. For instance, a hybrid material of carbon nanotubes (CNTs) immobilized on smectite clays was fabricated and employed on a membrane of perfluorosulfonic acid. A highly homogeneous nanocomposite membrane with outstanding mechanical properties was produced through a solution–precipitation method [42]. It possessed high efficacy in proton diffusion, ensured by a framework made up of long nanotubes distributed through the clay nanoplatelets activated by acid groups. The addition of this hybrid to polymers produced membranes with higher solidity and extended thermal stability at higher temperatures.

Even the dielectric properties of materials can be improved by forming such nanocomposites. Particularly, a composite of MWCNTs, polyvinylidene fluoride (PVDF), and clay was prepared via the melt-mixing method by a group of researchers [43]. They reported that the incorporation of 1.0 wt % clay into a MWCNT/PVDF nanocomposite with 0.5 wt % MWCNTs led to an increase of 670% in the dielectric permittivity and a reduction of 68% in the dissipation factor at 100 Hz.

Similarly, the elastic and electrical properties of such nanocomposites have been explored by different groups of scientists, using both computational [44] and experimental [45] methods. For improving electrical properties, a multiphase composite was manufactured based on thermosetting epoxy, multiwalled carbon nanotubes, and hydrotalcite clay. The DC conductivity measurement showed an electrical conductivity value of 2 S/m, achieved at the highest considered concentration of CNTs.

Scholars are also exploring the elastomeric nature of different clay–CNT composites. The hybridization of poly(diallyldimethylammonium chloride)-functionalized MWCNTs and hydroxyl-functionalized MMT showed an elastomeric nature [46]. Furthermore, the composite incorporated styrene–butadiene rubber (SBR) system and was successful in improving the dispersion with SBR latex.

Recently, a clay-based hybrid film fabricated with functionalized carbon nanotubes, sandwiched between smectite clay nanoplatelets through layer-by-layer deposition, has been reported [47]. Single-walled carbon nanotubes (SWCNTs) were covalently functionalized with phenol groups via 1,3-dipolar cycloaddition, which allows stable dispersion in polar media. A bottom-up approach and self-assembly helped in the production of hybrid thin films, where the Langmuir–Schaefer deposition technique was used.

However, the properties of thermoplastics—including physicochemical, mechanical, and thermal properties—have been influenced strongly by montmorillonite and carbon nanotubes acting as reinforcing particles for a long time. The improvement of their characteristics through the formation of nanocomposites has also been revealed by various researchers [48].

### 2.3. Polymer–Clay Nanocomposites

Apart from GO and CNTs, polymers are also widely utilized materials to make nanocomposites with clay. Very recently, polymer–clay nanocomposites have been developed to mitigate the water sensitivity of pure epoxy resin [49]. The inclusion of montmorillonite nanoclay in the epoxy results in reduced moisture absorption. Nanocomposites with 0.5, 1, and 1.5 wt % nanoclay were compared with pure epoxy in terms of their moisture absorption behavior. When the amount was 0.5 wt %, the nanocomposites performed better in distilled water, as it decreased the diffusion coefficient.

The improved mechanical properties of epoxy resin were also evaluated when nanoclay (NC), nano-graphene oxide (NGO), and carbon nanotubes with different weight percentages were immobilized in the epoxy [50]. The results showed that the NGO/epoxy nanocomposite had the lowest tensile strength, strain, and toughness, with more brittle behavior than the pure epoxy. The CNT/epoxy composite showed the highest ultimate strength but the lowest tensile strength.

It is important to use biodegradable materials. Hence, biodegradable plasticized cellulose acetate–clay hybrid nanocomposites represent such systems that can be classified as green materials [51]. They have been successfully synthesized from cellulose acetate, with triethyl citrate as a plasticizer and organically modified clay. The plasticizer concentration (15–40 wt %) was evaluated to check the nanocomposites' behavior.

The removal of Cr(VI) and Coomassie brilliant blue (CBB) from water has been explored with biopolymer–clay composites [52]. This involved the fabrication of hybrid adsorbents based on ceria, rice flour (the source of the biopolymer), and montmorillonite. The multilayer adsorption of CBB and Cr(VI) onto the composite surface was best illustrated by the Freundlich model. The sorption capacity for CBB and Cr(VI) is 713.513 and 182.037 mg g<sup>−1</sup>, respectively. The regeneration ability of three consecutive cycles made the hybrid effective.

To remove toxic ions such as Cr(VI) and Pb(II), a new attapulgite clay–carbon nanocomposite was synthesized by a one-pot hydrothermal process using attapulgite clay and glucose. This new nanocomposite exhibited maximum adsorption capacities of 177.74 and 263.83 mg g<sup>−1</sup> for Cr(VI) and Pb(II) ions, respectively [53].

Among others, chitosan–clay nanocomposites have the capability to remove water pollutants through effective adsorption processes. These nanocomposites have been found to adsorb ~99% of micropollutants from water, including dyes, metals, and harmful negative ions [54]. Moreover, ~94% of the targeted herbicides were successfully removed from the media of interest by this particular nanocomposite. There are a number of such chitosan-based clay nanocomposites that are applicable to wastewater treatment.

To make potential biomedical nanocomposites, the issue of cytotoxicity is always there to be addressed. One earlier work subjected copolymer/organoclay nanocomposites developed from co- and terpolymers such as poly(3,4-dihydro-2H-pyran-alt-maleic anhydride), poly(DHP-alt-MA), poly(3,4-dihydro-2H-pyran-co-maleic anhydride-co-vinyl acetate), and poly(DHP-co-MA-co-VA), along with bentonite clay, to cytotoxicity tests on L929 cells [55]. The MTT cell viability assay revealed that the nanocomposites could decrease cell viability. Thus, such nanocomposites may also be biocompatible for further work in biomedical areas.

Furthermore, some nanocomposites are employed in tissue engineering. Particularly, hydrogels and their derivatives are most useful in this case. A photo-crosslinkable chitosan hydrogel assisted by 2D nanoclay was reported to be effective for tissue generation [56]. The reinforced hydrogels activated the proliferation and induced the division of entrapped mesenchymal stem cells *in vitro*. Interestingly, the chitosan–montmorillonite hydrogels could direct native cells, thereby enhancing calvarial healing without any therapeutic agents or stem cells.

Film-based nanocomposites represent a good platform for dynamic purposes. A film of cellulose nanofibrils (CNFs) and montmorillonite (MTM) supported by surface charge was prepared. The CNFs, either with quaternary ammonium cations or carboxylate anions, interacted with MTM nanoplatelets with negative charges [57]. The impact of ionic charges of CNFs and their resultant interactions with MTM nanoplatelets is significant to understand the structure and mechanical properties of the nanocomposite films, as explained in the work.

Meanwhile, clay–polymer nanocomposites are also important for molecular loading and release, due to their high surface area. For example, bentonite–alginate nanocomposites are such materials with the capacity to load imidacloprid (an insecticide) and release it efficiently [58]. The basic composition involves the exfoliation of bentonite into nanoplatelets, followed by addition to the alginate hydrogel, resulting in significant effects on the architecture and release properties. It was noted that the time for 50% release ( $T_{50}$ ) of imidacloprid from the nanocomposite initially increased and reached a maximum at 10 wt % bentonites. At this point, the  $T_{50}$  value for the release of imidacloprid was 2.5 times that for its release from pure alginate.

For crop production, slow-release fertilizers (SRFs) are of utmost interest, because they can control the efficiency of nutrient utilization [59]. To overcome the issue of uncontrolled release of earlier fertilizers, a lignin–clay-nanohybrid-based double-layer SRF was formulated to slowly release nitrogen fertilizer, improving the water-holding capacity. For that, first, epoxypropyltrimethylammonium chloride (ETAC) and quaternary ammonium lignin (QAL) were prepared sequentially through a known protocol that was employed to obtain the SRF beads. Simple mixing of clay with the prepared QAL produced the lignin–clay nanohybrid. The positive charge on the QAL led to the insertion of lignin into the clay matrix. The hydrophobic lignin–clay nanohybrid was crosslinked with alginate, followed by a coating of the highly water-absorbent polymer poly(acrylic acid) (3% *w/v*) to form double-layer SRF beads. The produced fertilizer had a slower urea release rate than that of previously reported SRFs. The process of development of SRFs is shown below in Figure 3.

Nanocomposite films composed of sodium alginate/poly(vinyl alcohol)/montmorillonite clay were used to investigate the *in vitro* properties of the encapsulated antibiotic ceftriaxone sodium (CTX) [60]. The clay was employed as a nanofiller to improve their thermal stability and mechanical strength. A two-step discharge mode of the antibiotic was observed, with an early burst liberation from the *ex vivo* permeation. In fact, the sustained pH-dependent drug release could be explained from the dissolution studies of the drug-loaded nanocomposite.

Another polymer–clay nanocomposite was developed where low-density polyethylene was shown to form a composite with Laponite clay, which acted as a Pickering stabilizer [61]. The surfactant-free formation of polyethylene from range of polar and ionic comonomers was investigated to evaluate their influence on the formation mechanism and the stability

in both the presence and absence of Laponite. The stabilization efficiency offered by clay was dependent on the monomer present.



**Figure 3.** The synthesis procedure of double-layer SRFs using bio-based coating materials (reproduced from ref. [59]; copyright 2020 American Chemical Society).

The drawback of flexible polyurethane foam (PUF)—useful for bedding, transportation, and furniture—is its flammability [62]. To prevent this issue, an environmentally friendly and flame-retardant chitosan/vermiculite clay nanocoating was proposed for deposition on polyurethane foam through layer-by-layer assembly. The thermal shielding characteristic of this polymer/clay nanocoating makes this system user-friendly and enables the use of polyurethane foam for insulation applications.

One important application of clay-polymer nanocomposites is the formation of nanowalls that can restrict the passage of oxygen. These are formed as thin films of sodium montmorillonite clay with branched polyethylenimine (PEI) [63]. Oxygen transmission rates through these films decrease when the pH of the PEI increases.

#### 2.4. Carbon Dot–Clay Nanocomposites

Some of the other carbon-originated nanomaterials not discussed above, such as carbon dots or carbon quantum dots, are also well utilized to obtain clay-based nanocomposites with interesting properties. Carbon dots and nanoclusters are such materials, with dynamic applications. Our group has contributed in this area by developing photoreponsive carbon-dot-incorporated azobenzene nanocluster–clay (bentonite) hybrids with the ability to act as optoelectronic devices [64]. The complete scheme for the synthesis of these nanohybrids is shown in Figure 4 below. The basic scaffold of the nanocomposite was made up of azobenzene nanoclusters (AZO<sub>NC</sub>) and bentonite clay (BTN), which were characterized by electrochemical impedance spectroscopy. It was noted that doping with electron-rich carbon dots synthesized from cysteine and methionine (through pyrolysis) could enhance the AC conductivity of the resultant nanocomposites. Further tunability of the conductivity could be achieved in the presence of UV light, which was directly related to the UV-light-sensitivity of the AZO<sub>NC</sub>. The *trans*–*cis* isomerization of AZO<sub>NC</sub> under UV-365 might be the reason for such behavior of the nanocomposite. Ma et al. demonstrated the successful use of carbon dots (C-dots) and sheet-like hectorite clay as physical crosslinkers to fabricate C-dots–clay–poly(N-isopropylacrylamide) nanocomposite hydrogels (coded as C-dots–clay–PNIPAm hydrogels) [65]. The hydrogels were also endowed with fluorescence features that were associated with C-dots in the hydrogels. The as-fabricated C-dots–clay–PNIPAm hydrogels are promising for applications in sensors, biomedical

carriers, and tissue engineering. Hazarika et al. showed eco-friendly, high-performance, waterborne hyperbranched polyester nanocomposites with different doses of clay–carbon dot nanohybrids, fabricated for the first time through an in situ polymerization technique without any solvent or compatibilizing agent [66]. The nanocomposite was also used as a visible-light-active photocatalyst for the removal of organic dyes such as rhodamine B. In addition, the nanocomposite exhibited biodegradation behavior against *Pseudomonas aeruginosa* bacteria. Thus, this type of nanocomposite is an exceptionally promising candidate as an environmentally friendly, low-cost, and effective adsorbent for the elimination of contaminants from the atmosphere.

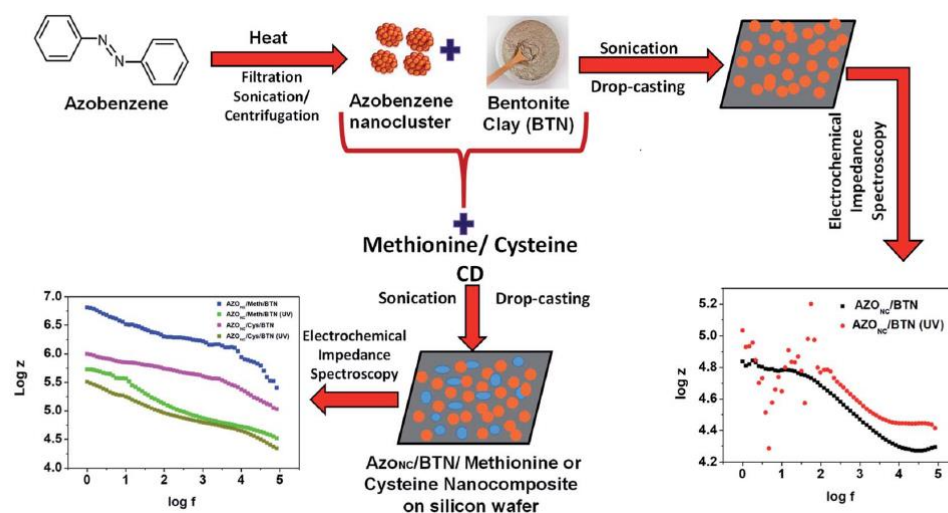


**Figure 4.** Protocol adopted to develop a photoresponsive carbon-dot-incorporated azobenzene nanocluster–clay (bentonite) hybrid with tunable conductivity (reproduced from ref. [64]; copyright 2020 Royal Society of Chemistry).

### 3. Summary and Conclusions

It has been demonstrated that clay materials have tremendous potential in all applications in combination with carbon nanomaterials. This review shows their improved properties and functions when in nanocomposite form. The main components from the carbon nano-domain are graphene and its derivatives, carbon nanotubes, polymers, carbon dots, and clusters, all of which have been used so far to make nanocomposites with clay. Particularly, the mechanical strength of the hybrid materials is greatly enhanced when clay is connected to carbon nanomaterials in the form of films or particles. In fact, molecular loading and controlled release can be better established in these nanocomposites as compared to pure clay materials. Their use in catalysis is outstanding owing to their increased surface area, providing space for reactions to take place with tunable reactivity. In the case of wastewater treatment to remove pollutants such as heavy metal ions or other toxins and dyes, these materials exhibit the desired efficacy. Responsivity to stimuli can be imparted to hybrid materials by various carbon nanomaterials with amazing optical and magnetic properties. This review constitutes a great platform to explore the latest findings on carbon-nanomaterial-based nanocomposites and will definitely help researchers to expand their knowledge further.

**Author Contributions:** Data curation, J.S.B.; writing—original draft preparation, J.S.B. and D.C.; writing—review and editing, J.S.B. and D.C.; All authors have read and agreed to the published version of the manuscript.

**Funding:** This research received no external funding.

**Conflicts of Interest:** The authors declare no conflict of interest.

## References

1. Guggenheim, S.; Martin, R.T. Definition report of clay and clay mineral: Joint the AIPEA and CMS nomenclature committees. *Clay Miner.* **1995**, *30*, 257–259. [[CrossRef](#)]
2. Guggenheim, S.; Adams, J.M.; Bain, D.C.; Bergaya, F.; Brigatti, M.F.; Drits, V.A.; Formoso, M.L.L.; Galan, E.; Kogure, T.; Stanjek, H. Summary of recommendations of nomenclature committees relevant to clay mineralogy: Report of the Association Internationale pour l'Etude des Argiles (AIPEA) Nomenclature Committee for 2006. *Clay Miner.* **2006**, *41*, 863–877. [[CrossRef](#)]
3. Ihekwe, G.O.; Shondo, J.N.; Orisekeh, K.I.; Kalu-Uka, G.M.; Nwuzor, I.C.; Onwualu, A.P. Characterization of certain Nigerian clay minerals for water purification and other industrial applications. *Heliyon* **2020**, *6*, e03783. [[CrossRef](#)]
4. Leonel, E.; Nassar, E.; Ciuffi, K.; Dos Reis, M.; Calefi, P. Effect of high-energy ball milling in the structural and textural properties of kaolinite. *Cerâmica* **2014**, *60*, 267–272. [[CrossRef](#)]
5. Abukhadra, M.R.; El-Meligy, M.A.; El-Sherbeeney, A.M. Evaluation and characterization of Egyptian ferruginous kaolinite as adsorbent and heterogeneous catalyst for effective removal of safranin-O cationic dye from water. *Arab. J. Geosci.* **2020**, *13*, 169. [[CrossRef](#)]
6. Hasan, A.K.M.M.; Dey, S.C.; Rahman, M.M.; Zakaria, A.M.; Sarker, M.; Ashaduzzaman, M.D.; Shamsuddin, S.M.D. A kaolinite/TiO<sub>2</sub>/ZnO-based novel ternary composite for photocatalytic degradation of anionic azo dyes. *Bull. Mater. Sci.* **2019**, *43*, 27. [[CrossRef](#)]
7. Ming, H. Modification of kaolinite by controlled hydrothermal deuteration—A DRIFT spectroscopic study. *Clay Miner.* **2004**, *39*, 349–362. [[CrossRef](#)]
8. Awwad, A.; Amer, M.; Al-aqarbeh, M. TiO<sub>2</sub>-kaolinite nanocomposite prepared from the Jordanian Kaolin clay: Adsorption and thermodynamics of Pb (II) and Cd (II) ions in aqueous solution. *Chem. Int.* **2020**, *6*, 168–178.
9. Schulze, D.G. Encyclopedia of soils in the environment. *Clay Miner.* **2005**, *1*, 246–254.
10. Hillier, S. On the mechanism of exfoliation of “vermiculite”. *Clay Miner.* **2013**, *48*, 563–582. [[CrossRef](#)]
11. Ombaka, O. Characterization and classification of clay minerals for potential applications in Rugi Ward, Kenya. *Afr. J. Environ. Sci. Technol.* **2016**, *10*, 415–431.
12. Ako, T.A.; Vishiti, A.; Ateh, K.; Kendia, A.C.; Suh, C.E. Mineral alteration and chlorite geothermometry in Platinum group elements(PGE)-Bearing meta-ultramafic Rocks from South East Cameroon. *J. Geosci. Geomat.* **2015**, *3*, 96–108.
13. Akisanmi, P. Classification of Clay Minerals. In *Mineralogy*; René, M., Ed.; IntechOpen: London, UK, 2022. [[CrossRef](#)]
14. Manukaji, J.U. An Investigation into the Use of Local Clays as a High Temperature Insulator for Electric Cookers. Ph.D. Thesis, Federal University of Technology, Minna, Nigeria, 2004.
15. Adamis, Z.; Williams, R.B.; Fodor, J. *Bentonite, Kaolin, and Selected Clay Minerals*; World Health Organization: Budapest, Hungary, 2005; Volume 9, pp. 56–63.
16. Steel, R.F.; Anderson, W. The interaction between kaolinite and Staphylococcus aureus. *J. Pharm. Pharmacol.* **1972**, *24*, 1–129.
17. Walsh, P.N. The effects of collagen and kaolin on the intrinsic coagulant activity of platelets. Evidence for an alternative pathway in intrinsic coagulation not requiring factor XII. *Br. J. Haematol.* **1972**, *22*, 393–405. [[CrossRef](#)] [[PubMed](#)]
18. Sengco, M.R.; Anderson, D.M. Controlling harmful algal blooms through clay Flocculation. *J. Eukaryot. Microbiol.* **2004**, *51*, 169–172. [[CrossRef](#)] [[PubMed](#)]
19. Wang, Y.; Guo, L.; Qi, P.; Liu, X.; Wei, G. Synthesis of three-dimensional graphene-based hybrid materials for water purification: A review. *Nanomaterials* **2019**, *9*, 1123. [[CrossRef](#)]
20. Winans, R.E.; Carrado, K.A. Novel forms of carbon as potential anodes for lithium batteries. *J. Power Sources* **1995**, *54*, 11–15. [[CrossRef](#)]
21. Kyotani, T. Synthesis of Various Types of Nano Carbons Using the Template Technique. *Bull. Chem. Soc. Jpn.* **2006**, *79*, 1322–1337. [[CrossRef](#)]
22. Meyers, C.J.; Shah, S.D.; Patel, S.C.; Sneeringer, R.M.; Bessel, C.A.; Dollahon, N.R.; Leising, R.A.; Takeuchi, E.S. Templated Synthesis of Carbon Materials from Zeolites (Y, Beta, and ZSM-5) and a Montmorillonite Clay (K10): Physical and Electrochemical Characterization. *J. Phys. Chem. B* **2001**, *105*, 2143–2152. [[CrossRef](#)]
23. Sonobe, N.; Kyotani, T.; Tomita, A. Formation of graphite thin film from polyfurfuryl alcohol and polyvinyl acetate carbons prepared between the lamellae of montmorillonite. *Carbon* **1991**, *29*, 61–67. [[CrossRef](#)]
24. Badosz, T.J.; Jagiello, J.; Putyera, K.; Schwarz, J.A. Pore Structure of Carbon—Mineral Nanocomposites and Derived Carbons Obtained by Template Carbonization. *Chem. Mater.* **1996**, *8*, 2023–2029. [[CrossRef](#)]
25. Kyotani, T.; Sonobe, N.; Tomita, A. Formation of highly orientated graphite from polyacrylonitrile by using a two-dimensional space between montmorillonite lamellae. *Nature* **1988**, *331*, 331–333. [[CrossRef](#)]
26. Sonobe, N.; Kyotani, T.; Tomita, A. Carbonization of polyfurfuryl alcohol and polyvinyl acetate between the lamellae of montmorillonite. *Carbon* **1990**, *28*, 483–488. [[CrossRef](#)]
27. Bakandritsos, A.; Steriotis, T.; Petridis, D. High Surface Area Montmorillonite Carbon Composites and Derived Carbons. *Chem. Mater.* **2004**, *16*, 1551–1559. [[CrossRef](#)]
28. Zhu, H.Y.; Vansant, E.F.; Lu, G.Q. Development of Composite Adsorbents of Carbon and Intercalated Clay for N<sub>2</sub> and O<sub>2</sub> Adsorption: A Preliminary Study. *J. Colloid Interface Sci.* **1999**, *210*, 352–359. [[CrossRef](#)]
29. Gogoi, J.; Choudhury, A.D.; Chowdhury, D. Graphene oxide clay nanocomposite as an efficient photo-catalyst for degradation of cationic dye. *Mater. Chem. Phys.* **2019**, *232*, 438–445. [[CrossRef](#)]

30. Zhang, E.; Wang, T.; Zhao, L.; Sun, W.; Liu, X.; Tong, Z. Fast Self-Healing of Graphene Oxide-Hectorite Clay-Poly(N,N-dimethylacrylamide) Hybrid Hydrogels Realized by Near-Infrared Irradiation. *ACS Appl. Mater. Interfaces* **2014**, *6*, 22855–22861. [[CrossRef](#)]
31. Zhang, R.; Alecrim, V.; Hummelgard, M.; Andres, B.; Forsberg, S.; Andersson, M.; Olin, H. Thermally reduced kaolin-graphene oxide nanocomposites for gas sensing. *Sci. Rep.* **2015**, *5*, 7676. [[CrossRef](#)]
32. Narayanan, D.P.; Gopalakrishnan, A.; Yaakob, Z.; Sugunan, S.; Narayanan, B.N. A facile synthesis of clay—Graphene oxide nanocomposite catalysts for solvent free multicomponent Biginelli reaction. *Arab. J. Chem.* **2020**, *13*, 318–334. [[CrossRef](#)]
33. Zhang, Z.; Luo, H.; Jiang, X.; Jiang, Z.; Yang, C. Synthesis of reduced graphene oxide-montmorillonite nanocomposite and its application in hexavalent chromium removal from aqueous solutions. *RSC Adv.* **2015**, *5*, 47408–47417. [[CrossRef](#)]
34. Srinivas, G.; Zhu, Y.; Piner, R.; Skipper, N.; Ellerby, M.; Ruoff, R. Synthesis of graphene-like nanosheets and their hydrogen adsorption capacity. *Carbon* **2010**, *48*, 630–635. [[CrossRef](#)]
35. Ruiz-García, C.; Pérez-Carvajal, J.; Berenguer-Murcia, A.; Darder, M.; Aranda, P.; Cazorla-Amorós, D.; Ruiz-Hitzky, E. Clay-supported graphene materials: Application to hydrogen storage. *Phys. Chem. Chem. Phys.* **2013**, *15*, 18635–18641. [[CrossRef](#)] [[PubMed](#)]
36. Liu, L.; Zhang, Y.; He, Y.; Xie, Y.; Huang, L.; Tan, S.; Cai, X. Preparation of montmorillonite-pillared graphene oxide with increased single- and co-adsorption towards lead ions and methylene blue. *RSC Adv.* **2015**, *5*, 3965–3973. [[CrossRef](#)]
37. Bakandritsos, A.; Simopoulos, A.; Petridis, D. Carbon Nanotube Growth on a Swellable Clay Matrix. *Chem. Mater.* **2005**, *17*, 3468–3474. [[CrossRef](#)]
38. Zhang, W.; Phang, I.Y.; Liu, T. Growth of Carbon Nanotubes on Clay: Unique Nanostructured Filler for High-Performance Polymer Nanocomposites. *Adv. Mater.* **2006**, *18*, 73–77. [[CrossRef](#)]
39. Wang, Z.; Meng, X.; Li, J.; Du, X.; Li, S.; Jiang, Z.; Tang, T. A Simple Method for Preparing Carbon Nanotubes/Clay Hybrids in Water. *J. Phys. Chem. C* **2009**, *113*, 8058–8064. [[CrossRef](#)]
40. Lan, Y.; Lin, J. Observation of Carbon Nanotube and Clay Micelle like Microstructures with Dual Dispersion Property. *J. Phys. Chem. A* **2009**, *113*, 8654–8659. [[CrossRef](#)]
41. Zhang, C.; Tjiu, W.W.; Liu, T.; Lui, W.Y.; Phang, I.Y.; Zhang, W. Dramatically Enhanced Mechanical Performance of Nylon-6 Magnetic Composites with Nanostructured Hybrid One-Dimensional Carbon Nanotube-Two-Dimensional Clay Nanoplatelet Heterostructures. *J. Phys. Chem. B* **2011**, *115*, 3392–3399. [[CrossRef](#)]
42. Simari, C.; Potsi, G.; Policicchio, A.; Perrotta, I.; Nicotera, I. Clay–Carbon Nanotubes Hybrid Materials for Nanocomposite Membranes: Advantages of Branched Structure for Proton Transport under Low Humidity Conditions in PEMFCs. *J. Phys. Chem. C* **2016**, *120*, 2574–2584. [[CrossRef](#)]
43. Khajepour, M.; Arjmand, M.; Sundararaj, U. Dielectric Properties of Multiwalled Carbon Nanotube/Clay/Polyvinylidene Fluoride Nanocomposites: Effect of Clay Incorporation. *Polym. Compos.* **2016**, *37*, 161–167. [[CrossRef](#)]
44. Thakur, A.K.; Kumar, P.; Srinivas, J. Studies on Effective Elastic Properties of CNT/Nano-Clay Reinforced Polymer Hybrid Composite. *IOP Conf. Ser. Mater. Sci. Eng.* **2016**, *115*, 012007. [[CrossRef](#)]
45. Egiziano, L.; Lamberti, P.; Spinelli, G.; Tucci, V.; Guadagno, L.; Vertuccio, L. Electrical Properties of Multiphase Composites based on Carbon Nanotubes and an Optimized Clay Content. *AIP Conf. Proc.* **2016**, *1736*, 020146.
46. Song, S.H. The Effect of Clay/Multiwall Carbon Nanotube Hybrid Fillers on the Properties of Elastomer Nanocomposites. *Int. J. Polym. Sci.* **2018**, *2018*, 5295973. [[CrossRef](#)]
47. Chalmpes, N.; Kouloumpis, A.; Zygori, P.; Karouta, N.; Spyrou, K.; Stathi, P.; Tsoufis, T.; Georgakilas, V.; Gournis, D.; Rudolf, P. Layer-by-Layer Assembly of Clay–Carbon Nanotube Hybrid Superstructures. *ACS Omega* **2019**, *4*, 18100–18107. [[CrossRef](#)]
48. Sanusi, O.M.; Benelfellah, A.; Hocine, N.A. Clays and carbon nanotubes as hybrid nanofillers in thermoplastic-based nanocomposites—A review. *Appl. Clay Sci.* **2020**, *185*, 105408. [[CrossRef](#)]
49. Muralishwara, K.; Sudhakar, Y.N.; Kini, U.A.; Sharma, S.; Gurumurthy, B.M. Moisture absorption and spectroscopic studies of epoxy clay nanocomposite. *Polym. Bull.* **2022**, *79*, 5587–5611. [[CrossRef](#)]
50. Adarmanabadi, S.R.; Jafari, M.; Farrash, S.M.H.; Heidari, M. Effect of nano clay, nano-graphene oxide and carbon nanotubes on the mechanical and tribological properties of crosslinked epoxy nanocomposite. *PLoS ONE* **2021**, *16*, e0259401. [[CrossRef](#)]
51. Park, H.M.; Misra, M.; Drzal, L.T.; Mohanty, A.K. “Green” Nanocomposites from Cellulose Acetate Bioplastic and Clay: Effect of Eco-Friendly Triethyl Citrate Plasticizer. *Biomacromolecules* **2004**, *5*, 2281–2288. [[CrossRef](#)]
52. Fakhar, N.; Khan, S.A.; Siddiqi, W.A.; Khan, T.A. Investigating the sequestration potential of a novel biopolymer-modified ceria/montmorillonite nanocomposite for chromium and Coomassie brilliant blue from the aqueous phase: Equilibrium and kinetic studies. *Environ. Sci. Adv.* **2022**, *1*, 558–569. [[CrossRef](#)]
53. Chen, L.F.; Liang, H.W.; Lu, Y.; Cui, C.H.; Yu, S.H. Synthesis of an Attapulgite Clay@Carbon Nanocomposite Adsorbent by a Hydrothermal Carbonization Process and Their Application in the Removal of Toxic Metal Ions from Water. *Langmuir* **2011**, *27*, 8998–9004. [[CrossRef](#)]
54. Biswas, S.; Fatema, J.; Debnath, T.; Rashid, T.U. Chitosan–Clay Composites for Wastewater Treatment: A State-of-the-Art Review. *ACS EST Water* **2021**, *1*, 1055–1085. [[CrossRef](#)]
55. Can, H.K.; Sevim, H.; Şahin, O.; Gürpınar, O.A. Experimental routes of cytotoxicity studies of nanocomposites based on the organo-bentonite clay and anhydride containing co- and terpolymers. *Polym. Bull.* **2022**, *79*, 5549–5567. [[CrossRef](#)]

56. Cui, Z.K.; Kim, S.; Baljon, J.J.; Wu, B.M.; Aghaloo, T.; Lee, M. Microporous methacrylated glycol chitosan- montmorillonite nanocomposite hydrogel for bone tissue engineering. *Nat. Commun.* **2019**, *10*, 3523. [[CrossRef](#)] [[PubMed](#)]
57. Xu, D.; Wang, S.; Berglund, L.A.; Zhou, Q. Surface Charges Control the Structure and Properties of Layered Nanocomposite of Cellulose Nanofibrils and Clay Platelets. *ACS Appl. Mater. Interfaces* **2021**, *13*, 4463–4472. [[CrossRef](#)] [[PubMed](#)]
58. Zhang, H.; Shi, Y.; Xu, X.; Zhang, M.; Ma, L. Structure Regulation of Bentonite-Alginate Nanocomposites for Controlled Release of Imidacloprid. *ACS Omega* **2020**, *5*, 10068–10076. [[CrossRef](#)] [[PubMed](#)]
59. Zhang, S.; Fu, X.; Tong, Z.; Liu, G.; Meng, S.; Yang, Y.; Helal, M.I.D.; Li, Y.C. Lignin—Clay Nanohybrid Biocomposite-Based Double-Layer Coating Materials for Controllable-Release Fertilizer. *ACS Sustain. Chem. Eng.* **2020**, *8*, 18957–18965. [[CrossRef](#)]
60. Bibi, S.; Mir, S.; Rehman, W.; Mena, F.; Gul, A.; Alaryani, F.S.S.; Alqahtani, A.M.; Haq, S.; Abdellatif, M.H. Synthesis and In Vitro/Ex Vivo Characterizations of Ceftriaxone-Loaded Sodium Alginate/poly(vinyl alcohol) Clay Reinforced Nanocomposites: Possible Applications in Wound Healing. *Materials* **2022**, *15*, 3885. [[CrossRef](#)]
61. Morgen, T.O.; Luttkhedde, H.; Mecking, S. Aqueous Dispersions of Ethylene Copolymers and Their Laponite Clay Nanocomposites from Free-Radical Dispersion Polymerization. *Macromolecules* **2019**, *52*, 4270–4277. [[CrossRef](#)]
62. Lazar, S.; Carosio, F.; Davesne, A.L.; Jimenez, M.; Bourbigot, S.; Grunlan, J. Extreme Heat Shielding of Clay/Chitosan Nanobrick Wall on Flexible Foam. *ACS Appl. Mater. Interfaces* **2018**, *10*, 31686–31696. [[CrossRef](#)]
63. Priolo, M.A.; Gamboa, D.; Grunlan, J.C. Transparent Clay Polymer Nano Brick Wall Assemblies with Tailorable Oxygen Barrier. *ACS Appl. Mater. Interfaces* **2010**, *2*, 312–320. [[CrossRef](#)]
64. Gogoi, J.; Shishodia, S.; Chowdhury, D. Tunable electrical properties of carbon dot doped photo-responsive azobenzene–clay nanocomposites. *RSC Adv.* **2020**, *10*, 37545–37554. [[CrossRef](#)] [[PubMed](#)]
65. Ma, S.; Zheng, H.; Chen, Y.; Zou, J.; Zhang, C.; Wang, Y. Nanocomposite Polymer Hydrogels Reinforced by Carbon Dots and Hectorite Clay. *J. Wuhan Univ. Technol.* **2020**, *35*, 287–292. [[CrossRef](#)]
66. Hazarika, D.; Karak, N. Nanocomposite of waterborne hyperbranched polyester and clay@carbon dot as a robust photocatalyst for environmental remediation. *Appl. Surf. Sci.* **2019**, *498*, 143832. [[CrossRef](#)]

**Disclaimer/Publisher’s Note:** The statements, opinions and data contained in all publications are solely those of the individual author(s) and contributor(s) and not of MDPI and/or the editor(s). MDPI and/or the editor(s) disclaim responsibility for any injury to people or property resulting from any ideas, methods, instructions or products referred to in the content.